NRIAG Journal of Astronomy and Geophysics 6 (2017) 300–310

Contents lists available at ScienceDirect

NRIAG Journal of Astronomy and Geophysics

journal homepage: www.elsevier.com/locate/nrjag

Full length article

Evaluation of optimal reservoir prospectivity using acoustic-impedance model inversion: A case study of an offshore field, western Niger Delta, Nigeria

Kehinde D. Oyeyemi [a,*], Mary T. Olowokere [b], Ahzegbobor P. Aizebeokhai [a]

[a] Applied Geophysics Unit, College of Science and Tech., Covenant University, Nigeria
[b] Department of Geology, Obafemi Awolowo University, Ile-Ife, Nigeria

ARTICLE INFO

Article history:
Received 23 July 2017
Revised 9 October 2017
Accepted 2 November 2017
Available online 11 November 2017

Keywords:
Acoustic impedance
Reservoir characterization
Seismic inversion
Hydrocarbon exploration
Niger Delta

ABSTRACT

The evaluation of economic potential of any hydrocarbon field involves the understanding of the reservoir lithofacies and porosity variations. This in turns contributes immensely towards subsequent reservoir management and field development. In this study, integrated 3D seismic data and well log data were employed to assess the quality and prospectivity of the delineated reservoirs (H1–H5) within the OPO field, western Niger Delta using a model-based seismic inversion technique. The model inversion results revealed four distinct sedimentary packages based on the subsurface acoustic impedance properties and shale contents. Low acoustic impedance model values were associated with the delineated hydrocarbon bearing units, denoting their high porosity and good quality. Application of model-based inverted velocity, density and acoustic impedance properties on the generated time slices of reservoirs also revealed a regional fault and prospects within the field.

1. Introduction

Determination of hydrocarbon bearing sands is a primary goal of most reservoir characterization projects and efforts are made to increase the confidence levels and reduce to the barest minimum the associated risks in drilling and exploration activities. Seismic inversion technique is principally a sophisticated process of inverting the seismic data into the elastic properties of the earth's subsurface. Elasticity and density are seismic characters of subsurface strata that are principally affected by the subsurface properties of rocks and fluids like lithology, porosity, fractures, textures, permeability, viscosity, fluid type and saturations (Mavko et al., 2009; Bosch et al., 2010). The quantitative characterization of these subtler fluid properties from seismic responses would go a long way to improve hydrocarbon reservoir characterization and reserve estimation within a hydrocarbon field (Russel, 1988; Doyen, 2007). Seismic inversion of the acoustic impedance property primarily involves the conversion of seismic traces into reflection coefficient time series, which are then converted back into acoustic impedance traces (Lavergne and Willim, 1977; Lindseth, 1979).

These generated acoustic impedance traces have the capacity to improve the accuracy of geological interpretations (e.g. environments of deposition and stratigraphy) and subsequent correlations with several petrophysical properties derived from the wireline logs (Xinyang et al., 2015). Benefits of seismic acoustic impedance data over conventional seismic data have been discussed by several researchers (Duboz et al., 1998; Connolly, 1999; Latimer et al., 2000; Yilmaz, 2001; Pendrel, 2006). Seismic inversion converts the seismic reflection data into an acoustic impedance section where band-limited seismic reflection data are transformed into quantitative rock properties for effective reservoir identification and description. Where the acquired exploration data involve high quality seismic and better distribution of well control, the interpretations of acoustic impedance model inversion often facilitates an improved estimation of reservoir porosity, acoustic impedance and uncertainty (Pendrel, 2001; Alshuhail et al., 2009;

* Corresponding author.
E-mail addresses: kdoyeyemi@yahoo.com, kehinde.oyeyemi@covenantuniversity.edu.ng (K.D. Oyeyemi).

Peer review under responsibility of National Research Institute of Astronomy and Geophysics.

Production and hosting by Elsevier

https://doi.org/10.1016/j.nrjag.2017.11.001
2090-9977/

Jalalalhosseini et al., 2015). Seismic acoustic impedance inversion section elucidates subsurface layers thereby enhancing visualization both in terms of layering and vertical resolution unlike reflection coefficient of raw seismic data that reveal only the interface. However, the major limitation of this method is that it suffers major setback when the reservoir thickness falls below a quarter of wavelength (1/4 λ). These thin beds and other small targets can be resolved on seismic data in two ways. The first involves increasing the dominant frequency of the stacked data simply by raising the bandwidth of the seismic data. The other involves conducting a phase shift or phase rotation of the seismic data through the use of advanced data processing algorithms and other inversion techniques such as seismic coloured inversion (Oyeyemi et al., 2016; Oyeyemi et al., 2017). The values of acoustic impedance derived from seismic inversion process are suitable to infer zones of high and low porosity within the delineated reservoirs. The relationship between the derived acoustic impedance and porosity is such that when the former is low, the later and the reservoir potential in terms of hydrocarbon saturation would be high (Dolberg et al., 2000; Farajpour et al., 2010; Çemen et al., 2014). Varela et al. (2006) reiterated the importance of acoustic impedance seismic inversion in reduction of uncertainty associated with reservoir production forecast, while Kadkhodaie-Ilkhchi et al. (2014) stated categorically that acoustic impedance section from a model-based seismic inversion technique is a robust tool for tight sandstone reservoir characterization. There are several methods for seismic inversion analysis and they are broadly categorized into either deterministic or stochastic process. The deterministic seismic inversion include band-limited, sparse-spike and model-based techniques. The focus of this study is to use a model-based deterministic seismic inversion technique to evaluate the hydrocarbon potential and prospectivity of the delineated reservoirs within the study area in western Niger Delta.

2. Geological setting

The hydrocarbon field of study is situated between Longitudes 5°00′E–5°02′E and Latitudes 5°50′N–5°52′N lying within the western parts of the continental margin shallow offshore Niger Delta basin (Fig. 1). The basin is bounded in the South by the Gulf of Guinea and in the North by the cretaceous tectonic elements including the Abakaliki uplifts, Afikpo syncline and the Anambra basin (Fig. 1). The siliciclastic deposits within this basin are of Tertiary age with three lithologic formations termed Akata, Agbada and Benin Formations (Fig. 2). The basal marine shale Akata Formation extends down to the basement and is a pro-delta shale unit with characteristic dark-grey and medium hard with floral fossils within its upper portion. The overlying paralic sequences of Agbada Formation house the oil and gas bearing reservoir units in Niger Delta; this geologic formation is composed of sandstone with interbeds of shale units that are typical of the delta front, distributaries channels and deltaic plain depositional facies (Avbovbo, 1978). Agbada Formation is characterized with increasing shale content from the upper to the lower portion denoting the seaward advance of the Niger Delta basin over some geologic time. The topmost Benin Formation is composed of massive continental plain sands that are highly porous with relatively low minor shale interbeds connoting an alluvial environment of deposition. The predominant structural styles within the Niger Delta are syn-sedimentary structures also referred to as the growth faults, deforming the delta under the Benin continental sandstone facies. These growth faults, generally trending in NE-SW and NW-SE directions (Hosper, 1971), are byproducts of that gravity sliding during the sedimentation of the deltaic deposits and they are polygenic in nature as their complexity increase in a down-dip direction of the delta (Merki, 1972; Corredor et al., 2005). According to Orife and Avbovbo (1982) the stratigraphic traps that are associated with unconformity surfaces

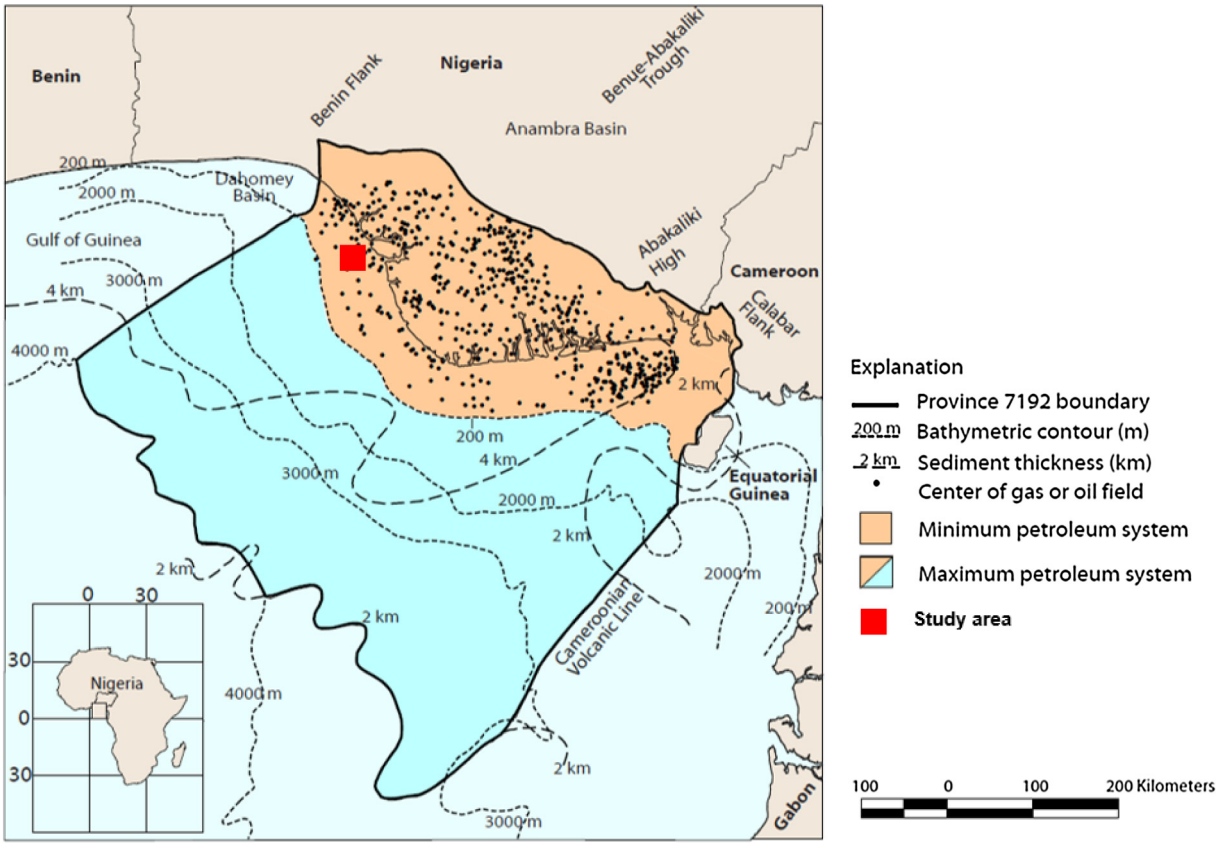

Fig. 1. Index map of the Niger Delta showing province outline bounding structural features and minimum petroleum system (After Michele et al., 1999).

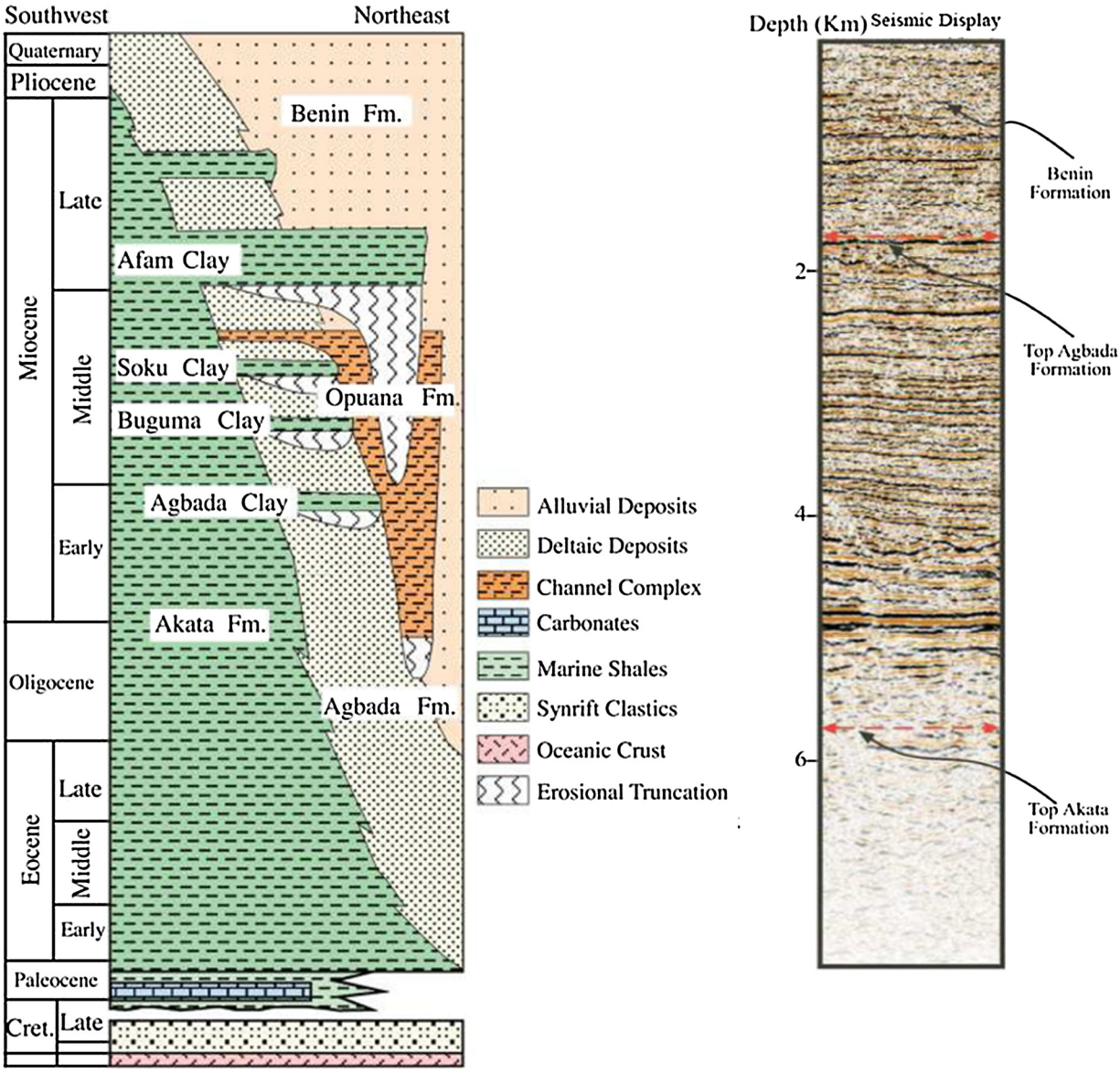

Fig. 2. Stratigraphy of the Niger Delta and variable density seismic display of the main stratigraphic units (Lawrence et al., 2002).

within the Niger Delta for oil and gas accumulations are paleochannel fills, crestal accumulations, sand pinch-outs, erosional truncations, canyons fills, incised valleys and lowstand fans. Shale intercalations or parasequence shale units within the Agbada Formation as shown in Fig. 2 have been interpreted to act as reservoir seals within the Niger Delta basin.

3. Seismic inversion

Acoustic impedance as a rock property is a product of density and velocity expressed by Eq. (1), both of which can be measured at well locations. Seismic data can also be expressed by Eq. (2) as the convolution of wavelet and reflection coefficient sequence. Where $S(t)$ is the synthetic seismic record, $W(t)$ is the seismic wavelet, $R(t)$ is the reflection coefficient series, and $N(t)$ is the random noise. Eq. (3) also shows the sequence of the reflection coefficient on normal incidence base on the assumption that the seismic incidence ray is perpendicular to the rock interface. Where R_i, V_i and ρ_i are the reflection coefficient, speed and density of the i^{th} layer.

$$Z_P = \rho V_P \tag{1}$$

$$S(t) = W(t) * R(t) + N(t) \tag{2}$$

$$R_i = \frac{\rho_i v_i - \rho_{i-1} v_{i-1}}{\rho_i v_i + \rho_{i-1} v_{i-1}} = \frac{Z_i - Z_{i-1}}{Z_i + Z_{i-1}} \tag{3}$$

In order to generate acoustic-impedance sections from seismic data, one of the major steps is to estimate the inverse wavelet $w(t)$ expressed by Eq. (4) which is used to ultimately build the initial model for seismic inversion (Fig. 1); where $a(t)$ and $\delta(t)$ are the inverse wavelet and unit impulse function respectively. The reflection coefficient $R(t)$ is obtained through a convolution process of seismic trace $S(t)$ and the inverse wavelet $a(t)$ as formulated in Eq. (5). Reconstruction of the P-impedance section is achieved by using a recursive method of estimating the reflection coefficient series $R(t)$ as stated in Eq. (6).

$$w(t) * a(t) = \delta(t) \tag{4}$$

$$R(t) = S(t) * a(t) \tag{5}$$

$$Z_{i+1} = \rho_{i+1} v_{i+1} = \rho_i v_i \frac{1+R_i}{1-R_i} = Z_i \frac{1+R_i}{1-R_i} \tag{6}$$

Model-based seismic inversion is a technique that involves the building of a geologically consistent model and then comparing the same model with measured seismic data. The results of the comparison between the observed data and modelled data are then used to iteratively update the model in such a way as to obtain a better match with the observed seismic data. Establishing the mathematical relationship between the initial model data and the seismic data along with the model update through iterations are resolved using two approaches such as application of the general linear inversion (Cook and Schneider, 1983) and the seismic lithologic modelling method based on the work of Gelfand and Larner (1984). The generalized linear inversion technique will compute the geological model that best fits the seismic data using a least squares method. The vector of k model parameters and vector of real data n observations are expressed by Eqs. (7) and (8). The relationship between the model and real data is then expressed in a functional form as shown in Eq. (9). Once this functional relationship is derived between both observed data and the models, any set of model parameters will generate an output. This obvious condition of non-uniqueness is eliminated within the generalized linear inversion merely by analyzing the error between the model output and observed data, the generated model parameters are subsequently perturbing so as to produce an output with inherent lesser error. This process would eventually lead the repeated iterations towards a satisfactory solution. This process can be expressed mathematically as Eq. (10).

$$M = (m_1, m_2, m_3, \ldots, m_k)^T \tag{7}$$

$$T = (t_1, t_2, t_3, \ldots, t_n)^T \tag{8}$$

$$t_i = F(m_1, m_2, \ldots m_k), \quad i = 1, \ldots, n. \tag{9}$$

$$F(M) = F(M_0) + \frac{\partial F(M_0)}{\partial M} \Delta M \tag{10}$$

The M_0 is the initial model, M is true earth model, ΔM is a change in model parameters, $F(M)$ is the seismic data (or observations), $F(M_0)$ is the calculated values from initial model, and $\frac{\partial F(M_0)}{\partial M}$ is

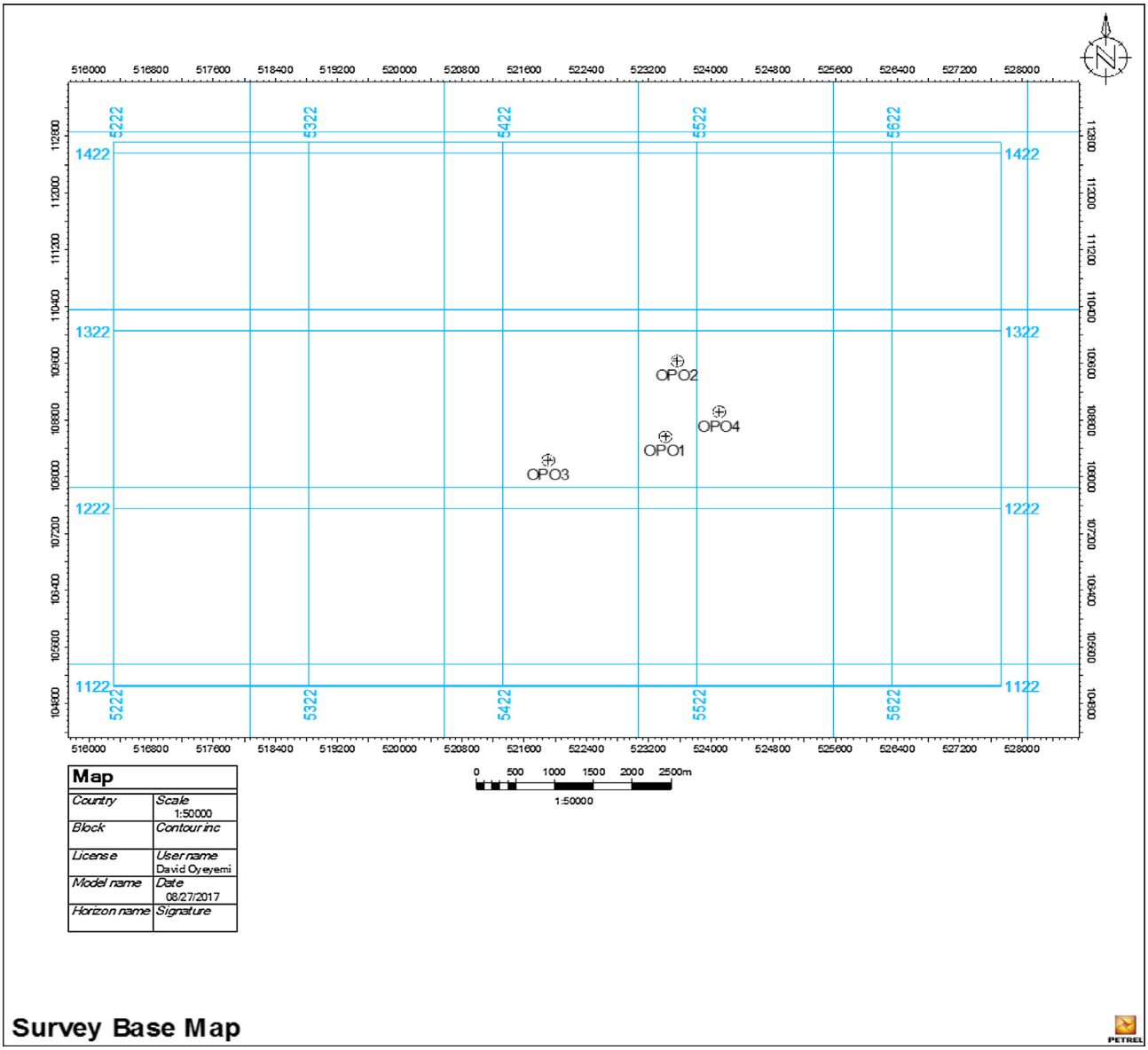

Fig. 3. Survey basemap in the study area showing the seismic survey profile lines (inlines and crosslines) and the available wireline logs.

change in the calculated values. The error between the observed data and the computed values is give as Eq. (11) which can be expressed in a matrix form in Eq. (12), where A is the matrix of derivatives with n-rows and k-columns. The solution to this matrix would appear as another matrix given as Eq. (13), and where A^{-1} is the inverse of the matrix A.

$$\Delta F = F(M) - F(M_0) \tag{11}$$

$$\Delta F = A\Delta M \tag{12}$$

$$\Delta M = A^{-1}\Delta F \tag{13}$$

Most times observed data than the model parameters ($n > k$), the matrix A is usually a non-square matrix and may not have a true inverse resulting to what is referred to as an overdetermined case. The above equation can be solve using least square solution expressed in Eq. (14).

$$\Delta M = (A^T A)^{-1} A^T \Delta F \tag{14}$$

4. Dataset and method

The geophysical data used for this research consist of poststack 3D seismic of 496 inlines and 780 crosslines with 3000 trace gathers and 751 samples per trace, covering an area of 83.45 km^2 and four digital suites of wireline logs designated as OPO 1–4 (Fig. 3). The depths of the wells range from 2438.4 m for OPO 2 to 2987.04 m for OPO 1. Density, sonic and porosity logs along with the checkshot and well-top data that were available for this research. Reservoir mapping and correlation were carried out using gamma-ray and resistivity logs motifs on the wireline logs. The 3D seismic data was time-migrated with good quality for horizon mapping and seismo-structural interpretation. Model-based seismic inversion technique, despite its inherent problem of non-uniqueness was adopted for this research because it could expedite better resolution compared to the band-limited and sparse-spike inversion techniques. The data preconditioning process was carried out using the procedures outlined by Veeken and Da Silva (2004) and the methodology workflow used for the seismic model-based inversion is presented in Fig. 4. The presented methodology has been attested to by several researchers to have high capacity of generating the subsurface structures from input geophysical data such that the resulting model fits the observation with some measure of reasonable error (Treitel and Lines, 2001). The input data comprising seismic and well-logging data were quality controlled to ensure that they were in suitable format for the seismic inversion.

The well data were calibrated with checkshot data with the sole intension of transforming the data from depth in well logs to time domain in seismic, thereby updating the sonic logs. The data from all the well logs, synthetic seismogram and the estimated reflection coefficient series were used for the extraction of seismic wavelet (Fig. 5). High correlation coefficients obtained between synthetic and real seismogram with minimal errors in all the wells location are presented in Fig. 6. The extracted statistical wavelet with zero phase was applied in order to align the reflections on the synthetic with the composite trace. The synthetic seismogram was then stretched and squeezed so as to make events on the synthetic tie with the events on the original seismic data. This process of seismic-to-well tie ultimately produced a new sonic logs, depth-time data logs and well synthetics that properly aligned with that of the seismic data. The synthetic seismogram generated from the field data is presented in Fig. 7. An initial model was later built using the low pass filtered acoustic impedance logs of the wells and the inversion process was then applied to the entire 3D seismic volume. The output of the final inversion results was thus well data constrained for better interpretation. The time slices of inverted

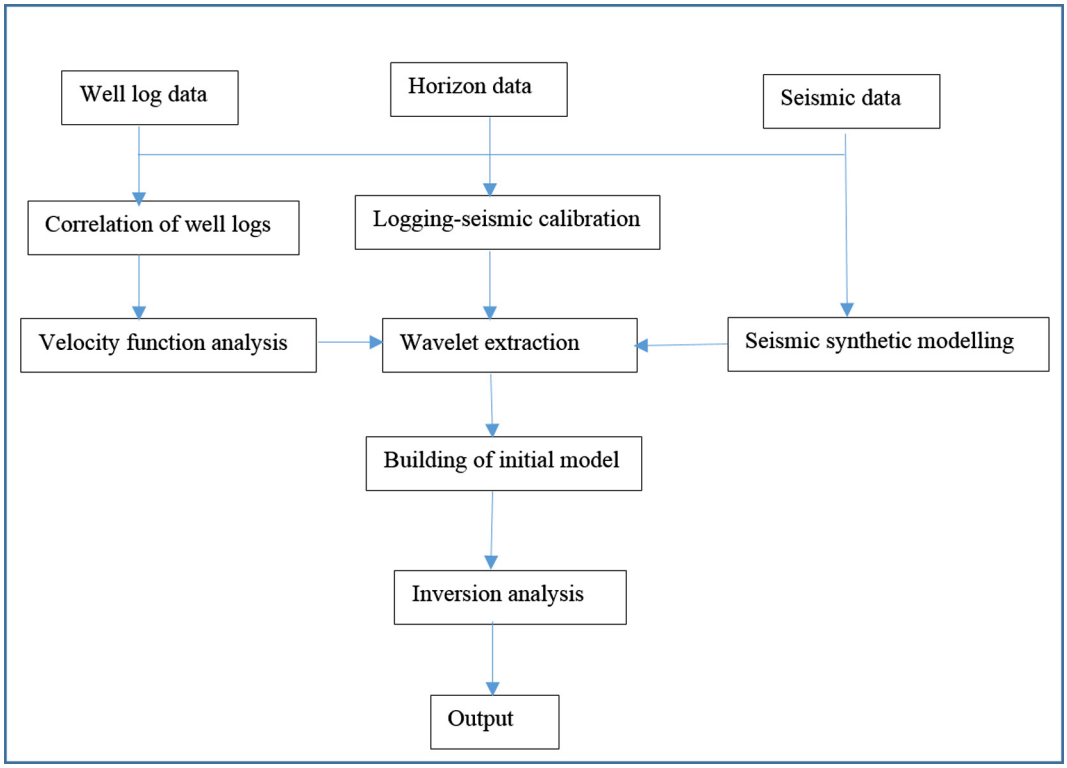

Fig. 4. Methodology workflow for the seismic inversion.

seismic window centered about the delineated horizons (reservoirs) were generated and evaluated based on the characteristic inverted elastic properties such as p-wave velocity, density, and acoustic impedance. These is necessary for both qualitative and quantitative analyses of the reservoirs prospectivity using the afore-stated relationships between the elastic properties and petrophysical properties such as volume of shale, porosity and fluid contents.

5. Results and discussion

The well logs correlation and analysis as presented in Fig. 7 reveal three lithofacies which are sand, sand-shale and shale facies. These lithofacies formed the sedimentary sequences within which identified hydrocarbon bearing reservoirs (H1–H5) were mapped and correlated across the entire wells (Fig. 7). Sand facies are porous strata that are impregnated with hydrocarbon, their pores are well interconnected and they are therefore permeable. Sand-shale facies are also porous and can accommodate hydrocarbon, but the fluid flow rate through these strata can be very slow as a results of shale intercalations. The pore spaces within the shale facies are not usually interconnected, having very low effective porosity and permeability. Hydrocarbon producibility of a clastic reservoir units such as in the Niger Delta basin can be greatly influenced by shale intercalations. The reservoir sand unit H1 on the well section correlation panel shows evidence of fewer shale intercalation compares to others (Fig. 7).

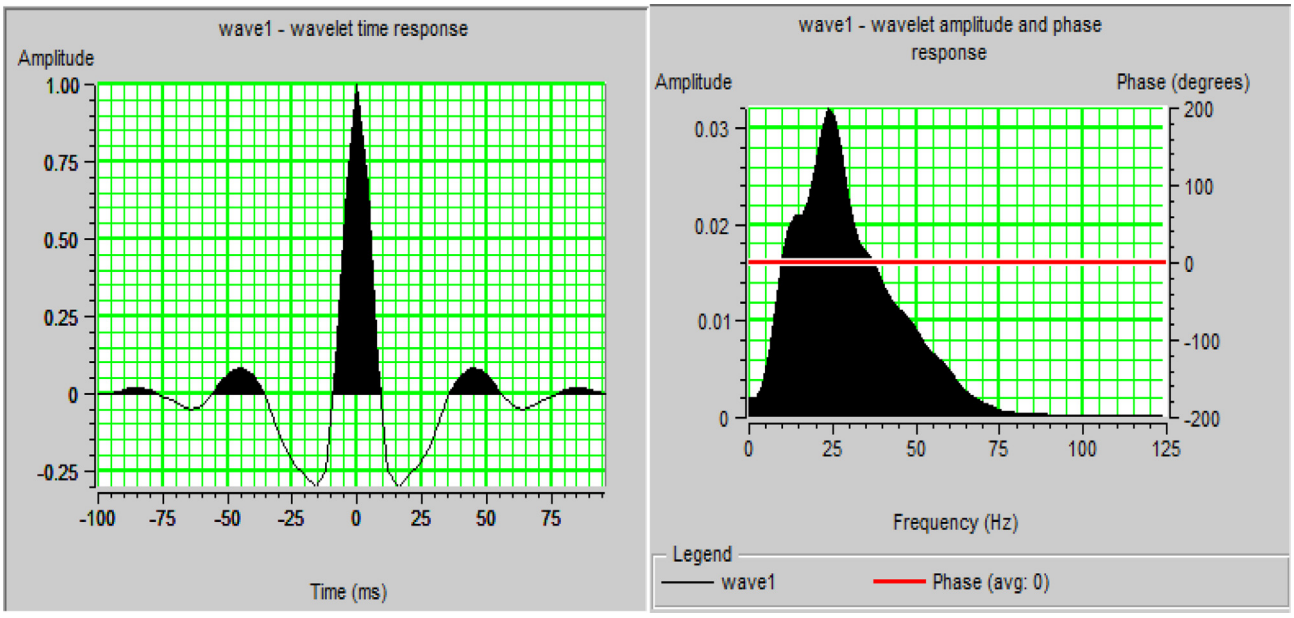

Fig. 5. Extracted statistical wavelet with zero phase from OPO 3.

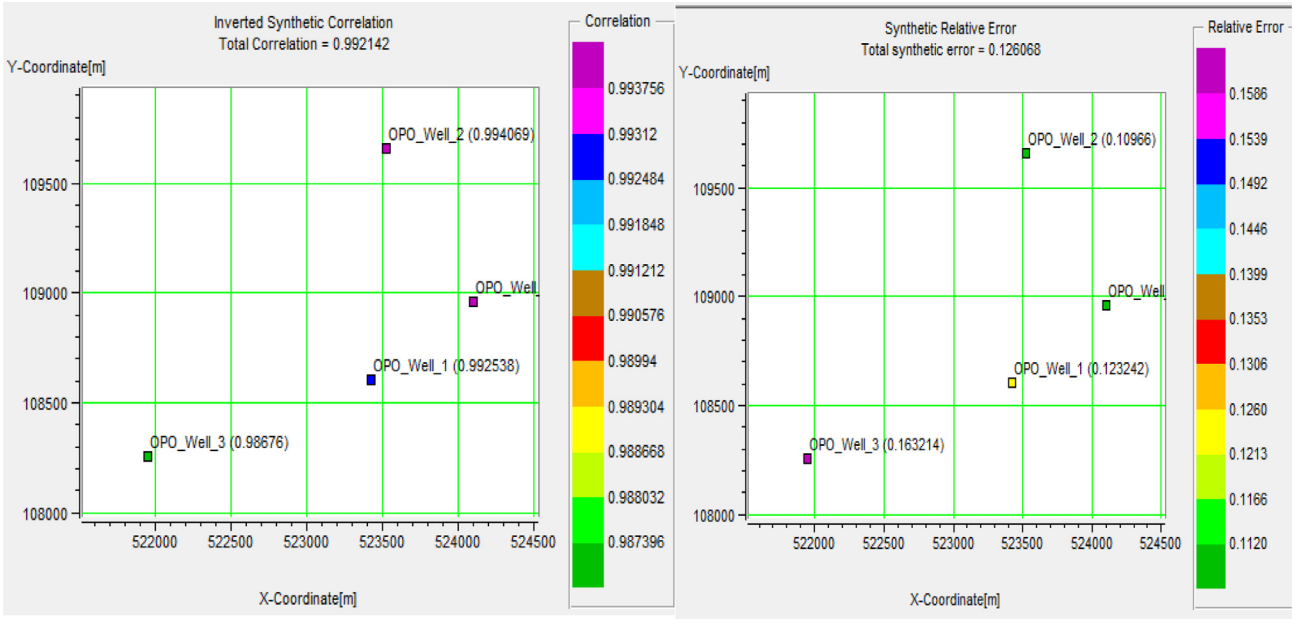

Fig. 6. Base maps for the synthetic correlation and relative error.

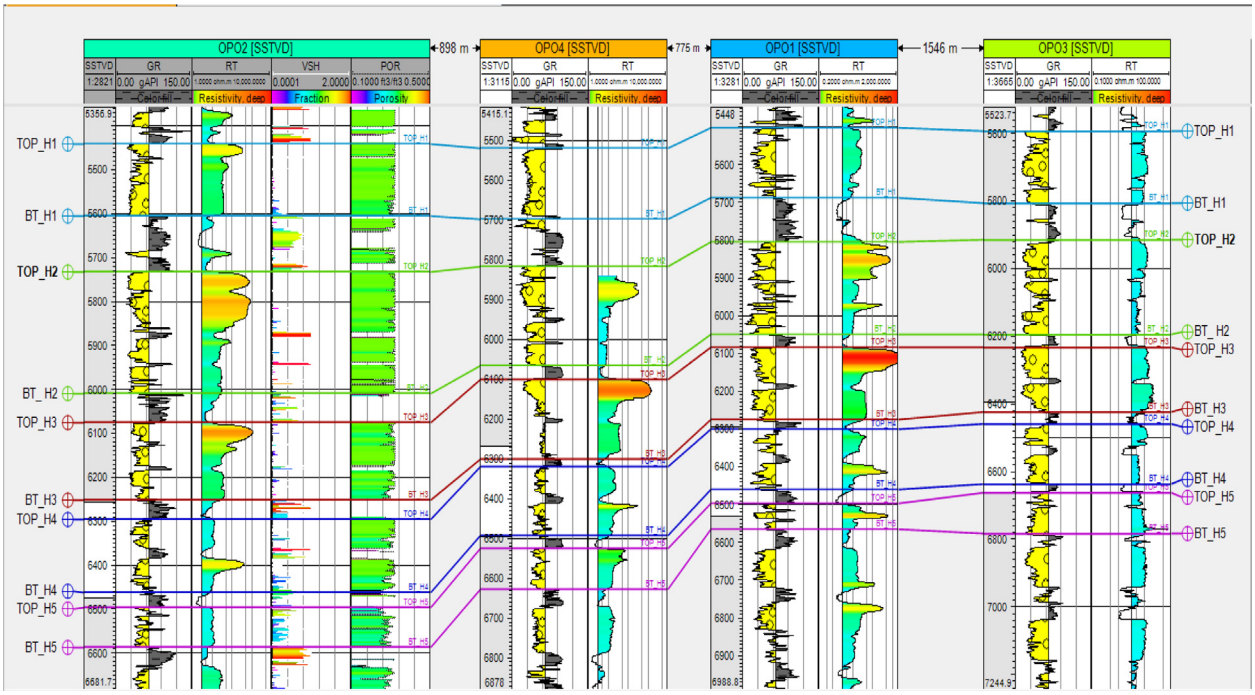

Fig. 7. NE-SW correlation of well logs and reservoir mapping.

Seismic inversion process is usually adopted to extract from seismic data the subsurface geology. This is done by estimating an interval impedance property from wireline logs data (sonic and density) which links directly to porosity from the seismic data. This is extremely important in that seismic inversion utilizes the power of both depth and spatial resolutions of the well logs and seismic data respectively (Veeken, 2007). The original seismic data and the initial model built are presented in Figs. 8 and 9. This initial model is the prior low frequency model generated from low pass filtered acoustic impedance logs from the wells and extrapolated along all the events in the seismic data. It is the absolute level of acoustic impedance for the seismic data. Four distinct sedimentary packages can be identified on the initial inversion model based on the acoustic impedance contrast. Boundaries between these layers and their internal lithologic contrasts are conspicuous; the first, second, third and fourth package extends from 800 to 1580 ms, 1580 to 2000 ms, 2000 to 2600 ms, and $\geqslant$2600 ms respectively. The five reservoirs H1–H5 are situated within the delineated second package from time 1620 to 2000 (ms) and the amplitude of the acoustic impedance values within this package is relatively low ranging from 19,396 to 22,383 ((ft/s)*(g/cc)). Low acoustic impedance values denotes a sand lithologic units with high porosity and hydrocarbon saturation. This line of interpreting porosity as well as fluid contents from acoustic impedance section has

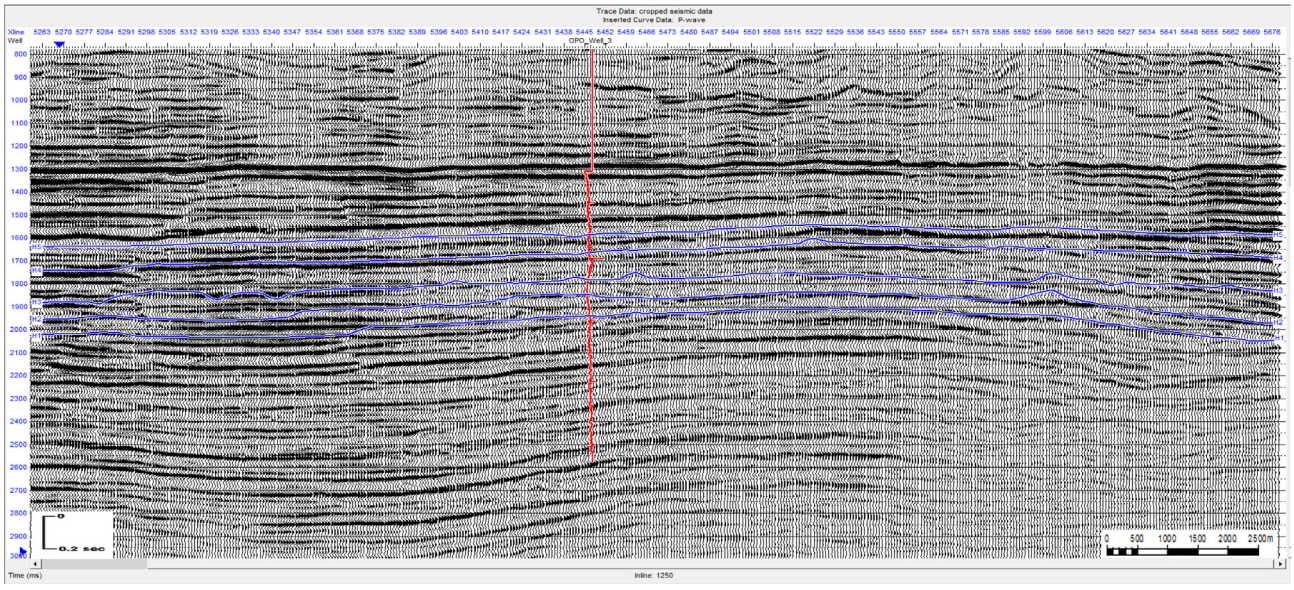

Fig. 8. Original 3D seismic data.

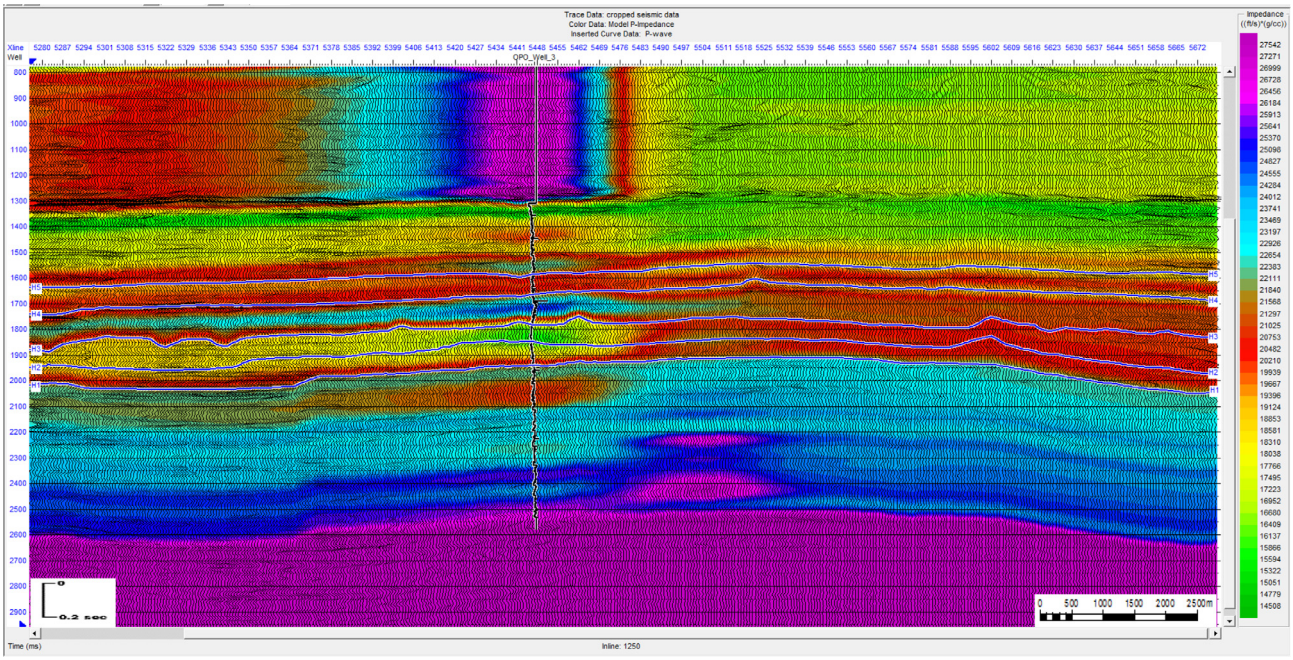

Fig. 9. Initial impedance model for seismic inversion analysis showing four distinct sedimentary packages toplap reflection termination against the sequence boundary.

contributed immensely to limiting exploration risks and hydrocarbon resource evaluation in challenging reservoirs (Latimer et al., 2000; Huuse and Feary, 2005; Çemen et al., 2014; Kadkhodaie-Ilkhchi et al., 2014; Farvour et al., 2015). The base of this sedimentary package can be interpreted as sequence boundary where there is a toplap termination of horizon from beneath at time 2100 (ms).

The final inverted seismic section which was obtained using the generalized linear inversion technique (Fig. 10). This technique involves several recursive iterative procedures of recalibrating the logs to seismic data in order to get an optimal wavelet that is used to convolve the initial acoustic impedance model such that the inversion error is drastically reduced. The final seismic inverted section reveals the variations in the sand and shale contents across all the delineated sedimentary packages (Fig. 10) based on the interpreted subsurface acoustic impedance properties. The topmost package coincides with the continental sand of Benin Formation and the high impedance values in some part of this package is not unconnected to the absence of wireline logs data within this area of the seismic section. The underlined second package shows evidence of high net-to-gross sand content with variable shale intercalations increasing from NW to SE portion of the seismic section. This sedimentary package is that of typical Agbada Formation with high potential for hydrocarbon bearing reservoirs that possess high porosity and hydrocarbon saturation. Beneath

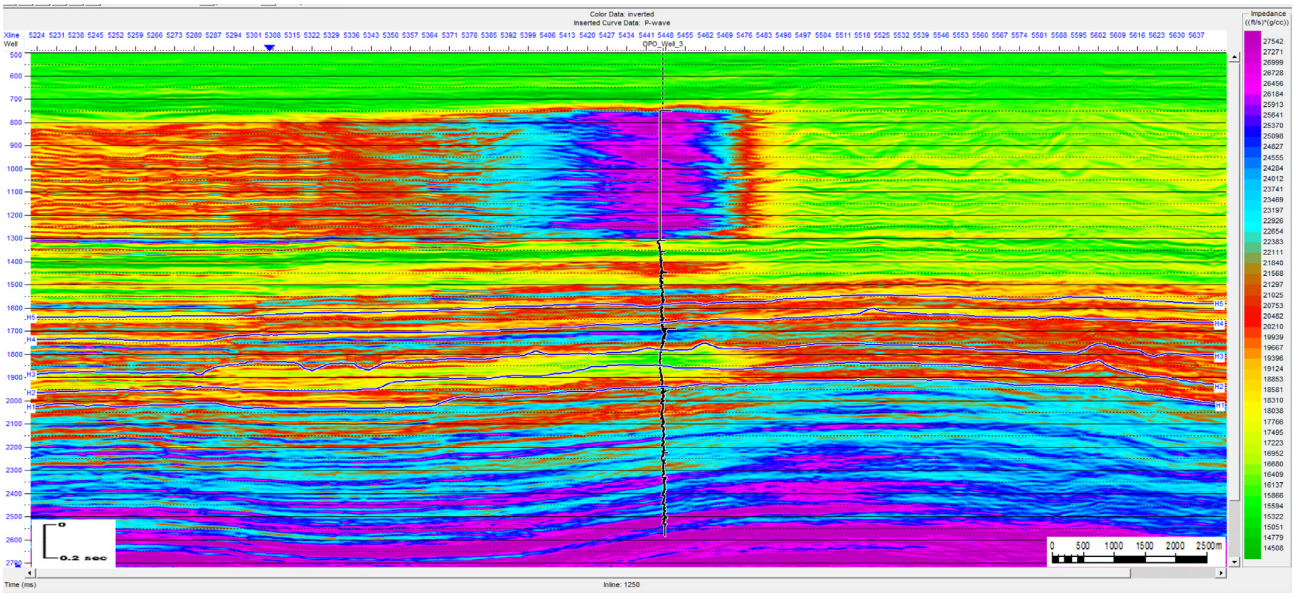

Fig. 10. Model-based acoustic impedance inversion of the 3D seismic data showing both vertical and lateral variations in subsurface acoustic impedance properties. All the delineated reservoir are within a sedimentary package with characteristic acoustic impedance.

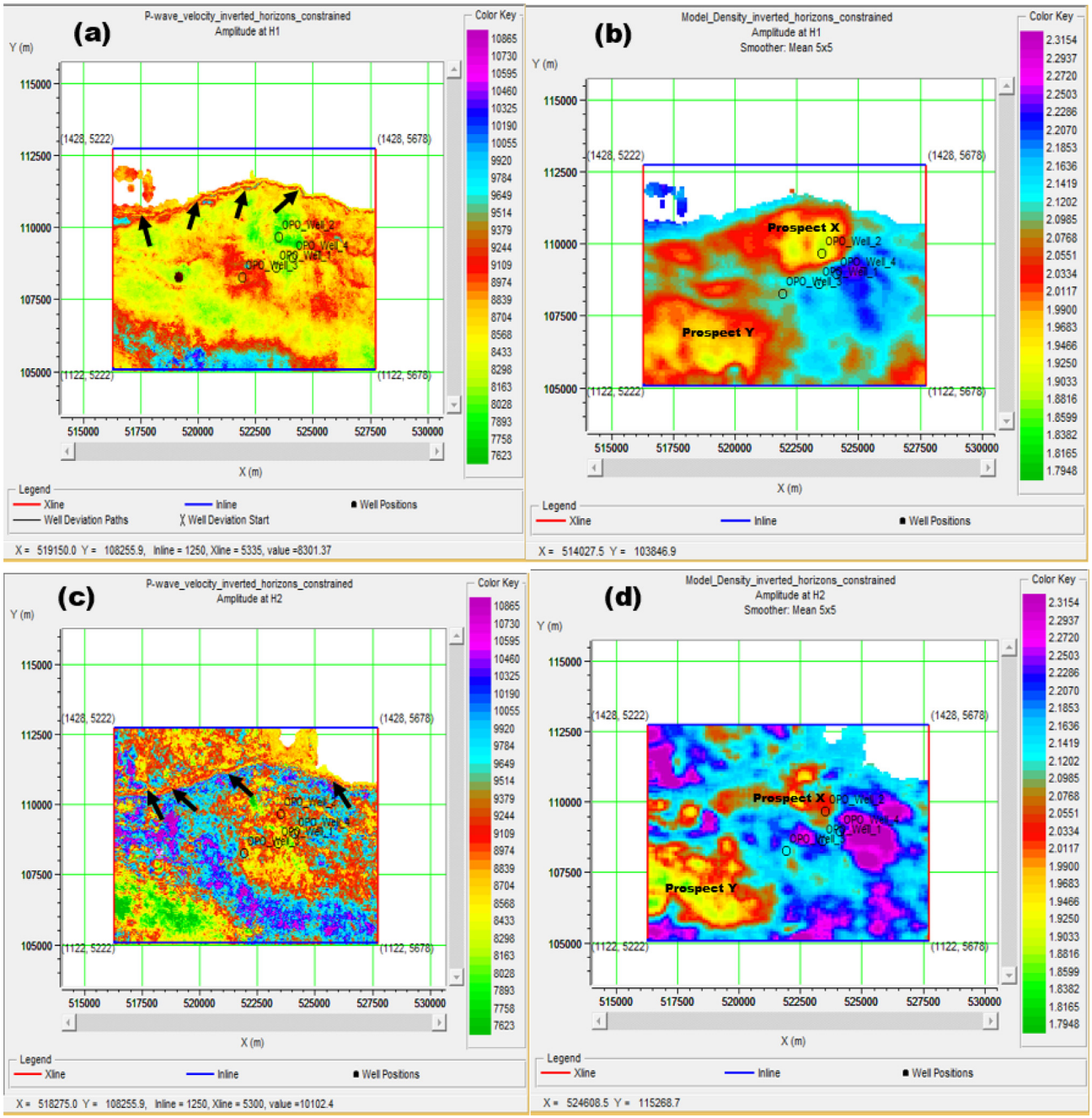

Fig. 11. Inverted P-wave velocity and density attributes over the time slice of the 3D seismic data corresponding to the delineated reservoir (a and b) H1 and (c and d) H2 on seismic section. The arrows show the presence of a regional fault delineated by p-wave velocity attributes.

this package is the basal unit of the Agbada Formation and the upper portion of the Akata Formation. This portion of the Niger Delta has been interpreted by some workers to be where the source rocks are situated (Evamy et al., 1978; Brownfield, 2016). The last sedimentary package is predominantly shale units with extremely high acoustic impedance values depicting very low to zero porosity values.

Fig. 11(a-d) shows the inverted model P-wave velocity and density for the 3D seismic time slice corresponding to both H1 and H2 reservoirs with the wells. The essence of these attributes was to delineate any prominent geologic structures and map the hydrocarbon prospects within the field. The P-wave velocity is predominantly low within the range of 7623–9244 (ft/s) for the reservoir sand H1, whereas the north-western to south-western portion of the same reservoir is predominantly low in the inverted model density (Fig. 9(a-b)). The range of inverted model p-wave velocity values within the portion of reservoir sand H2 where the wells are localized is between 8568 (ft/s) and 9244 (ft/s) which is quite low but is incomparable to that of the reservoir H1. A mappable regional fault is evident on the inverted p-wave velocity time slice maps for both H1 and H2 (Fig. 11a and c). The inverted model density for reservoir H2 is equally higher than that of the reservoir sand H1. These observation is basically tied to the shale contents of both reservoirs. Two prospect (X and Y) are identified as the area where there are high sand fairways within the field using inverted density attributes on the reservoirs (Fig. 11b and d). In terms of the

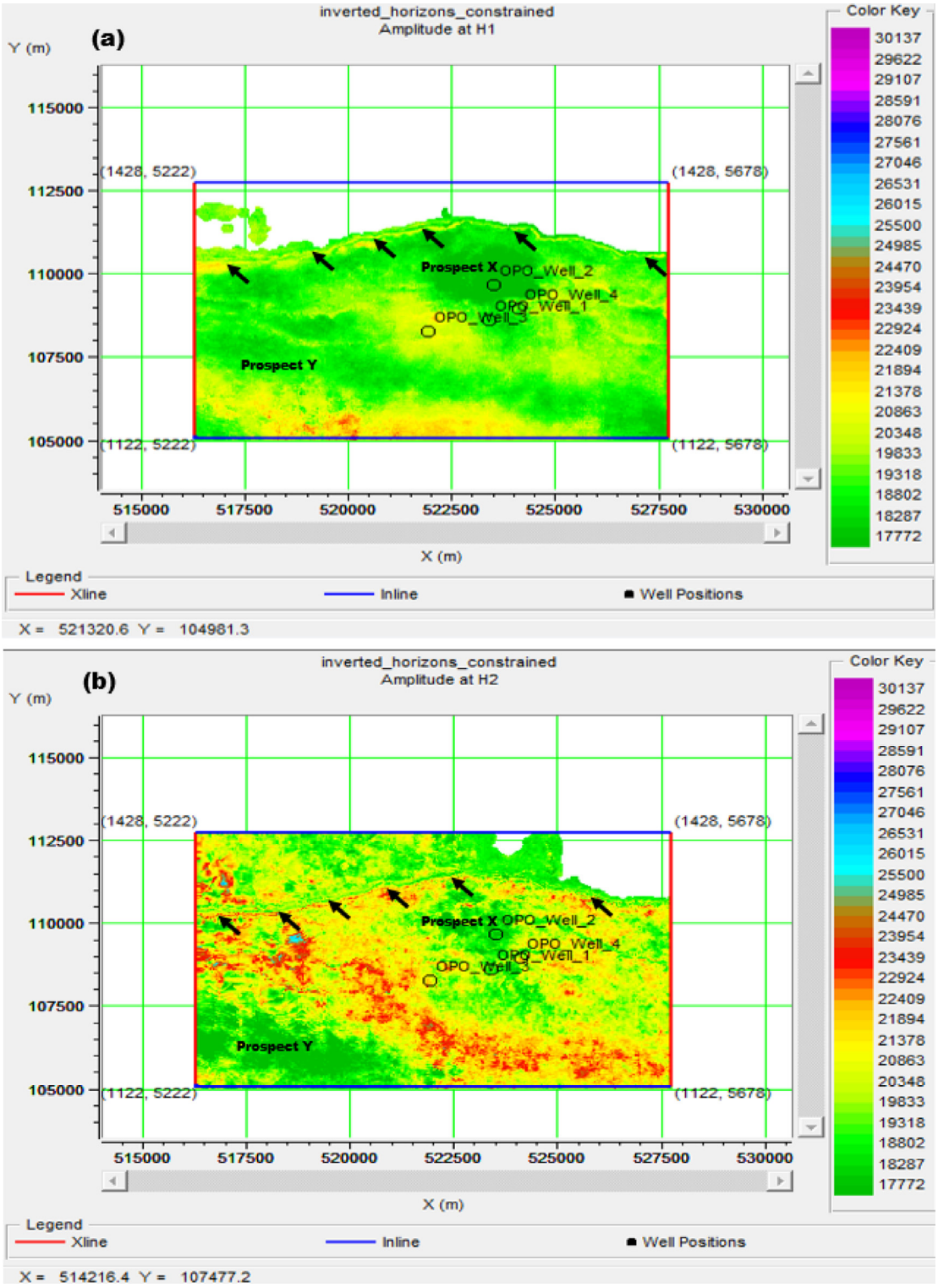

Fig. 12. Inverted acoustic impedance over time slices of 3D seismic section corresponding to the delineated reservoir (a) H1 and (b) H2. The arrows show the presence of a regional fault delineated by the acoustic impedance attribute.

model inverted acoustic impedance for the 3D seismic slices corresponding to the above reservoirs, sand H1 has lower impedance values than sand H2 as presented in Fig. 12(a-b), and this observations further affirm that reservoir H1 is cleaner (with low volume of shale) than reservoir H2. The portion within each reservoir time slice corresponding to the delineated prospects (X and Y) have characteristic low acoustic impedance denoting high porosity and fluid contents.

6. Conclusion

The following conclusions are drawn from the research:

(i) Inverted acoustic impedance model provides a better improved seismic attributes for accurate subsurface characterization and subsequent reservoir modelling than any the attributes derived from band-limited seismic data.

(ii) The generated impedance volume illuminates better the aerial and vertical distribution of the lithology and porosity. The output impedance volume equally yields credible estimations of these petrophysical properties away from well points.
(iii) The producing wells and delineated hydrocarbon bearing reservoirs fall within the area where the acoustic impedance values are low. Porosity and fluid saturation values in this area are characteristically high depicting a sand lithological units with intercalations of shale pockets.
(iv) The results of the acoustic impedance inversion would provide useful means of mitigating the risks associated with the exploratory efforts within the study area.

Acknowledgements

The authors wish to express their appreciations to the two reviewers and the editor for their efforts. We are grateful to the Nigerian department of petroleum resources (DPR) for providing us with the data used in this work. Also, a lot of thanks due to the Covenant University center for research innovation and development (CUCRID) for sponsoring this research.

References

Alshuhail, A., Lawton, D., Isaac, H., 2009. Acoustic Impedance Inversion of Vintage Seismic Data over a Proposed CO2 Sequestration Site in the Lake Wabamun Area, Alberta. CREWES Research Report, 21 (Chapter 1).

Avbovbo, A.A., 1978. Tertiary lithostratigraphy of Niger Delta. Am. Asso. Petrol. Geol. Bull. 62 (5), 297–306.

Brownfield, M.E., 2016. Assessment of undiscovered oil and gas resources of the Niger Delta province, Nigeria and Cameroon, Africa. In: Geologic Assessment of undiscovered Hydrocarbon of Sub-Saharan Africa by Brownfield, M.E. Digital Data Series 69–GG. U.S. Geological Survey, Reston, Virginia.

Bosch, M., Mukerji, T., Gonzalez, E.F., 2010. Seismic inversion for reservoir properties combining statistical rock physics and geostatistics: a review. Geophysics 75 (5). 75A165–75A176.

Çemen, I., Fuchs, J., Coffey, B., Gertson, R., Hager, C., 2014. Correlating porosity with acoustic impedance in sandstone gas reservoirs: examples from the Atokan sandstones of the Arkoma Basin, Southeastern Oklahoma. AAPG, Annual Convention Exhibition, Pittsburgh, Pennysylvania. Search and Discovery Article #41255.

Connolly, P., 1999. Elastic impedance. Lead. Edge 18 (4), 438–452. https://doi.org/10.1190/1.1438307.

Cook, D.A., Schneider, W.A., 1983. Generalized linear inversion of reflection seismic data. Geophysics 48 (6), 665–676.

Corredor, F., Shaw, J.H., Bilotti, F., 2005. Structural styles in the deepwater fold and Thrust belts of the Niger Delta. AAPG Bull. 89 (6), 753–780.

Dolberg, D.M., Helgesen, J., Hanssen, T.H., Magnus, I., Saigal, G., Pedersen, B.K., 2000. Porosity prediction from seismic inversion. Lavrans Field, Halten Terrace, Norway: Lead. Edge 19 (4), 392–399. https://doi.org/10.1190/1.1438618.

Doyen, P., 2007. Seismic Reservoir Characterization: An Earth Modelling Perspective: Houten. European Association of Geoscientists and Engineers Publication BV, Netherlands, p. 255.

Duboz, P., Lafet, Y., Mougenot, D., 1998. Moving to layered impedance cube: advantages of 3D stratigraphic inversion. First Break 17 (9), 311–318.

Evamy, B.D., Haremboure, J., Kamerling, P., Knaap, W.A., Molloy, F.A., Rowlands, P.H., 1978. Hydrocarbon habitat of Tertiary Niger Delta. Am. Asso. Petrol. Geol. Bull. 62, 277–298.

Farajpour, Z., Nabi Bidhendi, M., Torabi, M.R., Bagheri, M., 2010. Compare seismic inversion methods and result discussion in one of the oilfields in the south west of Iran. Presented at the 14th Iran Geophysical Conference.

Farvour, M., Yoon, W.J., Kim, J., 2015. Seismic attributes and acoustic impedance in interpretation of complex hydrocarbon reservoirs. J. Appl. Geophys. 114, 68–80. https://doi.org/10.1016/j.jappgeo.2015.01.008.

Gelfand, V.A., Larner, K.L., 1984. Seismic lithologic modeling. Lead. Edge 3 (11), 30–34.

Hosper, J., 1971. The geology of the Niger Delta area, in the Geology of the East Atlantic continental margin, Great Britain. Institute of Geological Science, Report, 70, No. 16, pp. 121–141.

Huuse, M., Feary, D.A., 2005. Seismic inversion for acoustic impedance and porosity of Cenozoic cool-water carbonates on the upper continental slope of the Great Australian Bight. Mar. Geol. 215, 123–134. https://doi.org/10.1016/j.margeo.2004.12.005.

Jalalalhosseini, S.M., Eskandari, S., Mortezazadeh, E., 2015. The technique of seismic inversion and use of the relation between inversion results and porosity log for predicting porosity of a carbonate reservoir in a South Iranian Oil Field. Energy Sources, Part ARecov., Util., Environ. Effects 37 (3), 265–272. https://doi.org/10.1080/15567036.2011.580326.

Kadkhodaie-Ilkhchi, R., Moussavi-Harami, R., Rezaee, R., Nabi-Bidhendi, M., Kadkhodaie-Ilkhchi, A., 2014. Seismic inversion and attributes analysis for porosity evaluation of the gas sandstones of the Whicher Range field in the Perth Basin, Western Australia. J. Nat. Gas Sci. Eng. 21, 1073–1083. https://doi.org/10.1016/j.jngse.2014.10.027.

Latimer, R.B., Davison, R., Van Riel, P., 2000. Interpreter's guide to understanding and working with seismic derived acoustic impedance data. Lead. Edge 19 (3), 242–256.

Lawrence, S.R., Munday, S., Bray, R., 2002. Regional geology and geophysics of the eastern Gulf of Guinea (Niger Delta to Rio Muni). Lead. Edge 21, 1112–1117.

Lavergne, M., Willim, C., 1977. Inversion of seismograms and pseudo velocity logs. Geophys. Prospect. 25 (2), 231–250. https://doi.org/10.1111/j.1365-2478.1977.tb01165.x.

Lindseth, R.O., 1979. Synthetic sonic logs—a process for stratigraphic interpretation. Geophysics 44 (1), 3–26.

Mavko, G., Mukerji, T., Dvorkin, J., 2009. The Rock Physics Handbook. Cambridge University Press.

Merki, P., 1972. Structural geology of the Cenozoic Niger Delta. In: Dessauvagie, T.F., Whiteman, A.J. (Eds.), African Geology. Ibadan University Press, pp. 636–646.

Michele, L.W., Tuttle, R., Charpentier, R., Michael, E.B., 1999. The Niger Delta Petroleum System: Niger Delta Province, Nigeria, Cameroon, and Equatorial Guinea. U.S. Geologic Survey, 35 pp.

Orife, J.M., Avbovbo, A.A., 1982. Stratigraphic and unconformity traps in the Nige Delta. In: Halbouty, M.T. (Ed.), The Deliberate Search for Subtle Trap. American Association of Petroleum Geologists Memoir, NY, pp. 251–265.

Oyeyemi, K.D., Aizebeokhai, A.P., Olowokere, M.T., Ayinde, O., 2016. Seismic-driven Reservoir Characterization, Offshore Niger Delta, Nigeria. SEG Technical Program Expanded Abstract 2016, pp. 2841–2845.

Oyeyemi, K.D., Olowokere, M.T., Aizebeokhai, A.P., 2017. Hydrocarbon resource evaluation using combined petrophysical analysis and seismically derived reservoir characterization, offshore Niger Delta. J. Explor. Prod. Technol. https://doi.org/10.1007/s13202-017-0391-6.

Pendrel, J., 2001. Seismic inversion—the best tool for reservoir characterization. CSEG Rec. 26 (1), 16–24.

Pendrel, J., 2006. Seismic inversion—a critical tool in reservoir characterization. Scand. Oil Gas Mag. 5 (6), 19–22.

Russel, B.H., 1988. Introduction to Seismic Inversion Methods. Course Notes Series, No. 2. S. N. Domenico Ed. Society of Exploration Geophysicists, Tulsa, Oklahoma. http://dx.doi.org/10.1190/1.978156802303.

Treitel, S., Lines, L., 2001. Past, present, and future of geophysical inversion—a new millennium analysis. Geophysics 66 (1), 21–24. https://doi.org/10.1190/1.1444898.

Varela, O.J., Torres-Verdin, C., Lake, L.W., 2006. On the value of 3D seismic amplitude data to reduce uncertainty in the forecast of reservoir production. J. Petrol. Sci. Eng. 50, 269–284. https://doi.org/10.1016/j.petrol.2005.11.004.

Veeken, P.C.H., 2007. Seismic stratigraphy, basin analysis and reservoir characterization. Seismic Exploration, vol. 37. Elsevier, Amsterdam.

Veeken, P.C.H., Da Silva, M., 2004. Seismic inversion methods and some of their constraints. First Break 22 (6), 47–70.

Xinyang, D., Jiyu, L., Yuchao, C., Fan, L., 2015. A study on seismic inversion method for identification of sand. IOSR J. Eng. 5 (8), 38–43.

Yilmaz, O., 2001. Seismic Data Analysis, vols. 1 and 2. Society of Exploration Geophysicists, Investigations in Geophysics, 10, Tulsa, SEG, 2027.